# The effect of porphyrins suspended with different electronegative moieties on the photovoltaic performance of monolithic porphyrin-sensitized solar cells with carbon counter electrodes

Jiangzhao Chen, Songguk Ko, Linfeng Liu, Yusong Sheng, Hongwei Han, Xiong Li*

*Michael Grätzel Center for Mesoscopic Solar Cells, Wuhan National Laboratory for Optoelectronics,*

*Huazhong University of Science and Technology, Wuhan 430074, Hubei, P. R. China*

∗ Correspondence to: Xiong Li (Email address: lxwhu2008@hotmail.com)

Tel: +86 27 87793027; fax: +86 27 87793027

## Abstract

Three D-π-A porphyrin sensitizers attached with different electronegative moieties (2,4,6-triphenyl-1,3,5-triazine, carbazole and triphenylamine) at the meso-position were designed and synthesized for monolithic dye-sensitized solar cells based on mesoscopic carbon counter electrodes. The effects of these different electronegative moieties on the photophysical, electrochemical and accordingly photovoltaic performance of the corresponding devices were investigated systematically. Electrochemical measurement indicates that the HOMO and LUMO energy levels could be tuned through introducing different electronegative groups onto the backbone of D-π-A porphyrin molecules. Current–voltage characteristics indicate that the $J_{sc}$ and $V_{oc}$ of the DSSCs based on **WH-C3**, **WH-C4** and **WH-C5** increase as electron-donating ability of their donors enhance in the order of **WH-C3** < **WH-C4** < **WH-C5** and **WH-C5**-sensitized cell showed the best photovoltaic performance: a short circuit photocurrent density ($J_{sc}$) of 11.43 mA cm$^{-2}$, an open circuit voltage ($V_{oc}$) of 633.84 mV, and a fill factor (*FF*) of 0.69, corresponding to an overall conversion efficiency ($\eta$) of 5.00%.

*Keywords:* Porphyrin dyes; Different electronegative moieties; Monolithic dye-sensitized solar cells; Carbon counter electrodes

## 1. Introduction

With the depletion of fossil fuels and exacerbation of pollution problems, dye-sensitized solar cells (DSSCs) as a promising photovoltaic device have attracted extensive attention owing to their high power conversion efficiency, ease of fabrication and potential low cost compared with traditional silicon-based solar cells.[1-5] It is well known that DSSCs are principally composed of dye-sensitized working electrodes (WE), electrolytes, and counter electrodes (CEs)，where the dyes play a crucial role in determining the power conversion efficiencies (PCEs) of the devices. In the past two decades, Rupolypyridyl sensitizers with PCEs of over 11%[6-9] have been demonstrated to be very efficient due to their broad absorption spectrum through metal-to-ligand charge transfer (MLCT), longer exciton lifetime, and long-term chemical stability.[2, 5, 10] However, several drawbacks, which include the high cost of noble metal ruthenium, the requirement for careful synthesis, tricky purification steps and low molar extinction coefficient,[10-12] and so on, restrict Rupolypyridyl sensitized DSSCs towards commercial viability. Seeking alternative snsetizers seems to be a solution to these problems, which is an intensive research topic of high priority.

As a promising substitute for the Rupolypyridyl dye in DSSCs, porphyrins have been widely investigated because of their low cost, high molar extinction coefficients and structural diversity.[13-19] Great progress has been made in the past few years and a record efficiency as high as 12.3% has been achieved by molecular engineering methodology based on cosensitization of porphyrin**YD2-o-C8** with organic dye **Y123** and a Cobalt (II/III) redox electrolyte.[20] Additionally, the solar cell cosensitized by organic dye **C1** and the porphyrin **XW4** with an extended conjugation framework and a carbazole donor exhibited a high PCE of 10.45% with an improved current density ($J_{sc}$) and an open-circuit voltage ($V_{oc}$) values.[21] Recently, through inserting a benzothiadiazole unit between the porphyrin ring and benzoic acid accepter, an structure-optimized dye **SM315** was obtained and produced a world record efficiency of 13% in the field of DSSCs.[22]

As similar as the structures of the most organic dyes, the porphyrin dyes are designed according to basic structures of Donor-π-conjugated bridge-Acceptor (simplified as D-π-A) which are beneficial to intramolecular electron transportation. In case of organic dyes, the donor is of great importance in determining the photovoltaic performance of DSSCs through influencing the photophysical and electrochemical properties of the sensitizers. Hence, various kinds of organic groups, such as triphenylamine,[23, 24] carbazole,[25, 26] coumarin,[27, 28] indoline,[29, 30] phenothiazine,[31-33] and so on, have been extensively applied as donors in organic dyes for DSSCs over the past two decades. On the contrary, literature investigating the influence of different donors on the photovoltaic performance of porphyrin-sensitized DSSCs was limited.[34]

In order to improve further the performance of porphyrin sensitized solar cells, more insight should be devoted into the structure-property relationships of this kind of dye. Herein, we designed and synthesized a serials of porphyrin dyes through incorporating different electronegative organic moieties (2,4,6-triphenyl-1,3,5-triazine, triphenylamine and carbazole) onto the dye molecule. Accordingly, the influence of different donors on the photophysical and electrochemical characteristics of porphyrin sensitizers were systematically investigated. It was found that different electronegative organic moieties significantly influence the HOMO, LUMO levels and molar absorption ability of porphyrin molecules. To further scrutinize the relationship between the electronegativity of organic moieties and the photovoltaic performance of DSSCs sensitized by the corresponding porphyrin dyes, a fully printable low-cost monolithic architecture with mesoscopic carbon counter electrodes was utilized to fabricate the complete DSSC devices. Thereinto, utilizing the porphyrin dye molecule (coded as **WH-C5**) attached with triphenylamine as donor afforded DSCs exhibiting a open circuit voltage ($V_{oc}$) of 633.84 mV, short-circuit current density ($J_{sc}$) of 11.43 mA cm$^{-2}$, fill factor (FF) of 0.69 and the best PCE of 5%.

## 2. Results and discussion

### 2.1. Synthesis

In the present work, three porphyrin dyes with different electronegative moieties (2,4,6-triphenyl-1,3,5-triazine, carbazole and triphenylamine) at the meso-position opposite to the anchoring benzoic acid group were designed and synthesized for monolithic DSSCs based on carbon/graphite counter electrodes, coded as **WH-C3**, **WH-C4** and **WH-C5**, respectively. The structures of the dyes and the synthetic scheme are shown in Fig. 1 and in Scheme 1, respectively. The detailed synthetic procedures are presented in the experimental section. The molecular structures of all target porphyrins and intermediates were confirmed by $^{1}H$ NMR, $^{13}C$ NMR and APCI/ESI-MS, which are given in the experimental section.

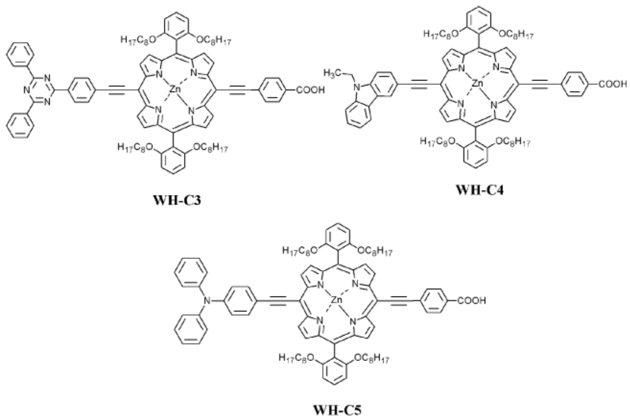


**Fig. 1** Molecular structures of sensitizers in this study.

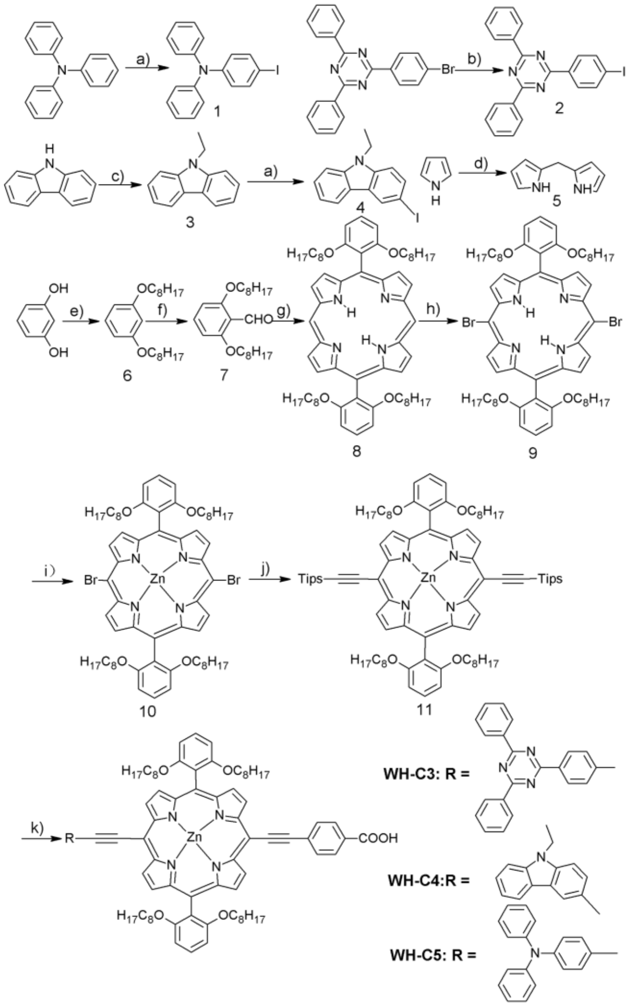

**Scheme 1**. Synthetic route of **WH-C3**, **WH-C4** and **WH-C5**. Reaction conditions: a) KI, $KIO_3$, $CH_3COOH$, 118℃; b) CuI, NaI, ethylenediamine, dioxane, 110 ℃, 24 h; c) bromoethane, KOH, DMF; d) HCHO,$CF_3COOH$, RT, 15min; e) 1-Bromooctane, $K_2CO_3$, acetone, 60℃, 4d; f) (ⅰ) n-butyllithium, TMEDA, THF, 0℃, 3h; (ⅱ) DMF, RT, 2h; g) (ⅰ) **5** , $CF_3COOH$, $CH_2Cl_2$, RT, 4h; (ⅱ) DDQ, 1h; h) NBS, pyridine, $CHCl_3$, 0 ℃, 0.5h; i) $Zn(OAc)_2$ $2H_2O$, Methanol/$CH_2Cl_2$, RT, 3h; j) (triisopropylsilyl)acetylene, $Pd(PPh_3)_2Cl_2$, CuI, triethylamine, THF, 65℃, 6h; k) (ⅰ) TBAF in THF, THF, RT, 0.5h; (ⅱ) **1**/**2**/**4**, 4-Iodobenzoic acid, $Pd_2(dba)_3$, $AsPh_3$, triethylamine, THF, 65℃, 5-8h.

## 2.2. Optical properties

The UV-vis absorption spectra of **WH-C3**, **WH-C4** and **WH-C5** in THF solution are depicted in Fig. 2. The corresponding peak positions and molar absorption coefficients (ε) of Soret and Q bands are listed in Table 1. As shown in Fig. 2, the three sensitizers exhibit typical porphyrin absorption characteristics with a strong Soret band appearing in the range of 400-500nm and mild Q bands appearing in the longer wavelength range of 600-700nm, which is attributed to π-π* charge transfer transitions of the conjugated molecule and intramolecular charge transfer (ICT) transitions of the D-π-A conjugated backbone. [35] According to the absorption data in Table 1, it is observed obviously that the Soret band and Q band peak positions for **WH-C4** and **WH-C5** are red-shifted in comparison with **WH-C3**, which may be ascribed to stronger electron-donating ability of carbazole and triphenylamine corresponding to the band gap ($E_{0\text{-}0}$) of three porphyrin dyes. Compared with **WH-C3** and **WH-C5**, it is clear that the maximum molar extinction coefficients of Soret band of **WH-C4** is the highest reaching 444300 $M^{-1}cm^{-1}$ which is roughly double that of **WH-C5**. Meanwhile, Fig. 3 presents the UV-visible absorption spectra of the sensitizers adsorbed on $TiO_2$ films. In comparison with the absorption spectra in solution, the trend of the Soret and Q bands in the absorption spectra is similar to when the sensitizers are adsorbed on $TiO_2$ films. Nevertheless, the Soret and Q absorption bands are broadened and red-shifted conspicuously. This phenomenon is proposed to result from the formation of J-aggregation.[13, 27, 36] Additionally, the fluorescent emission spectra were measured in THF and are shown in Fig. 4. For the fluorescence spectra, major emission bands are observed at 668, 671 and 673 nm for **WH-C3**, **WH-C4** and **WH-C5**, respectively, which are similar to the trend of the Soret band absorption spectra. Therefore, it can be concluded that porphyrin dye molecules with different kinds of donors possess significantly different optical properties.

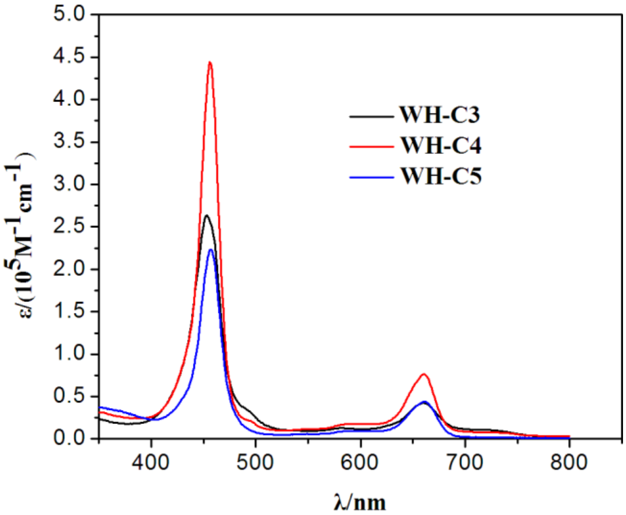


**Fig. 2** UV-visible absorption spectra of sensitizers in THF solvent.

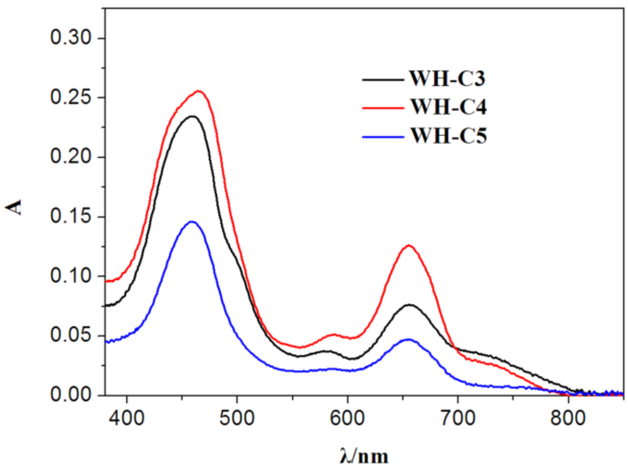


**Fig. 3** UV-visible absorption spectra of the sensitizers adsorbed on $TiO_2$ films.

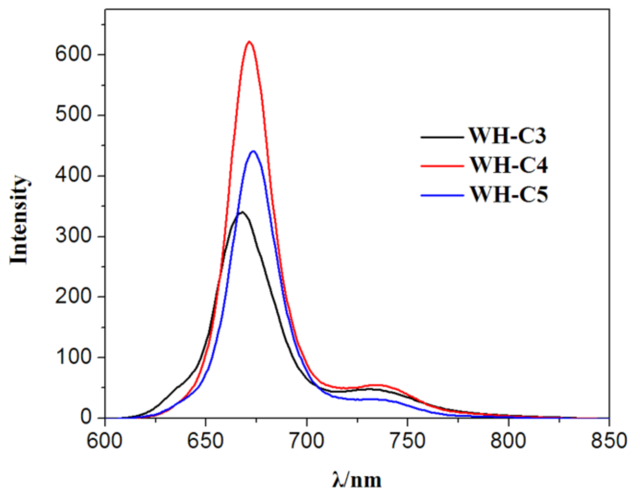


**Fig. 4** Emission spectra of sensitizers in THF solvent.

**Table 1.** Photophysical and electrochemical properties of the sensitizers.

| Dye | $\lambda_{max}$[a] /nm ($\varepsilon/10^4 M^{-1}cm^{-1}$) | Emission [a]$\lambda_{max}$ /nm | $E_{ox}$[b]/V(vs. NHE) | $E_{0-0}$[c] /V(vs. NHE) | $E_{LUMO}$[d]/V( vs. NHE) | Dye loading[e]/$10^{-7}$ $molcm^{-2}$ |
|---|---|---|---|---|---|---|
| **WH-C3** | 453(26.35),660(4.21) | 668 | 0.956 | 1.985 | -1.029 | 0.32 |
| **WH-C4** | 456(44.43),660(7.59) | 671 | 0.861 | 1.920 | -1.059 | 0.37 |
| **WH-C5** | 457(22.31),661(4.39) | 673 | 0.660 | 1.915 | -1.255 | 0.37 |

[a] Absorption and emission data were measured in THF at 25 ℃. Excitation wavelengths: 453 nm (**WH-C3**), 456 nm (**WH-C4**), 457nm (**WH-C5**). [b] The first porphyrin-ring oxidation was performed at 25℃ with each porphyrin (0.5 mM) in THF containing $TBAPF_6$(0.1M) under $N_2$ condition with a GC working electrode, a Pt counter electrode, and a Ag/AgCl reference electrode with a scan rate of 50 mV $s^{-1}$. [c] $E_{0-0}$ was estimated from the intersection wavelengths of the normalized UV/Vis absorption and fluorescence spectra. [d] $E_{LUMO} = E_{ox} - E_{0-0}$. [e] The amount of porphyrin dyes were carried out through the desorption of a 5 um thick $TiO_2$ film sensitized by

dye in the 0.05 M solution of NaOH in THF/EtOH/$H_2O$(v/v/v, 1:1:1) for 2 days.

**2.3. Electrochemical properties**

In order to investigate the feasibility of electron injection and dye regeneration processes in DSSCs, Cyclic voltammetry measurements for the three dyes were performed in water-free THF containing 0.1 M tetrabutylammonium hexafluorophosphate ($TBAPF_6$) as the supporting electrolyte at room temperature and cyclic voltammograms are presented in Fig. 5. It is observed that the electrochemical data for the three dyes displays quasi-reversible couples. The highest-occupied molecular orbitals (HOMOs) of dyes corresponding to the first redox potential were calculated to be 0.956, 0.861 and 0.660V for **WH-C3**, **WH-C4** and **WH-C5**, respectively. Practically, it was confirmed that $\eta_{inj}$ with unit efficiency requires approximately 0.2 V of over-potential ($-\Delta G$) between the $TiO_2$ conduction band (CB) and lowest unoccupied molecular orbital (LUMO) level of the dye, and 0.3 V of $-\Delta G$ between the highest occupied molecular orbital (HOMO) level of the dye and redox potential of the electrolyte, to create a sufficient driving forces for the electron injection from the dye to the CB of $TiO_2$ and the regeneration of oxidized dye.[5, 37] It is observed that the HOMO levels of the three porphyrin dyes are sufficiently more positive than the iodine/iodide redox potential value (0.4 V vs. NHE),[38] guaranteeing the efficient regeneration of oxidized dye through $I^-$ presented in the electrolyte of the DSSCs. The zero–zero excitation energies ($E_{0-0}$) were calculated to be 1.985V (**WH-C3**), 1.920V (**WH-C4**) and 1.915V (**WH-C5**) by the intersection of the normalized UV-vis absorption spectrum and steady-state fluorescence emission spectrum. The lowest-unoccupied molecular orbitals (LUMOs) levels of all porphyrin sensitizers were determined according to the expression of LUMO = HOMO - $E_{0-0}$ and the corresponding level values are summarized in Table 1. Obviously, the LUMO levels of all dyes are sufficiently more negative compared with the conduction band edge level ($E_{cb}$) of the $TiO_2$ electrode (-0.5 V vs. NHE), which means that electron injection from the excited dye into the conduction band of $TiO_2$ is thermodynamically feasible. Therefore, the three dyes are properly used as sensitizers for DSSCs.

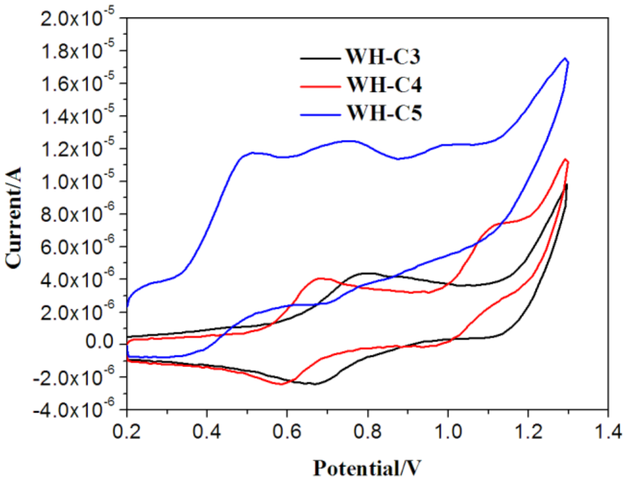


**Fig. 5** Cyclic voltammograms of sensitizers in THF at a scan rate of 50 mV/s at room temperature with 0.1 M tetra-n-butylammoniumhexafluorophosphate($TBAPF_6$) as the supporting electrolyte. GC working electrode, Pt wire counter electrode, and Ag/AgCl reference electrode were used.

**2.4. Photovoltaic performance of DSSCs**

In this work, we synthesized three porphyrin dyes with the incorporation of three different donors to investigate the effect of different donors on photovoltaic performance of monolithic dye-sensitized solar cells with mesoscopic carbon counter electrodes. Compared with the conventional DSSC, this monolithic DSSC permits printing paste layer by layer on a single FTO glass substrate by screen-printing technique, which makes large scale commercial production possible. Furthermore, carbon black/graphite composite used as counter electrodes in this study is an abundantly available and low-cost material compared with high cost metallic CE, which have been applied successfully in DSSCs.[39-41]

Monochromatic incident photon-to-current conversion efficiency (IPCE) for DSSCs is expressed as follows:[5, 42]

$$\mathrm{IPCE}(\lambda) = \eta_{\mathrm{LHE}}\eta_{\mathrm{inj}}\eta_{\mathrm{cc}}$$

Where $\eta_{\mathrm{LHE}}$ is the light harvesting efficiency, $\eta_{\mathrm{inj}}$ is the electron injection yield from the photo-excited dye into $TiO_2$, and $\eta_{\mathrm{cc}}$ is the charge collection efficiency at the electrodes. Among them, $\eta_{\mathrm{LHE}}$ and $\eta_{\mathrm{inj}}$ contribute to the improvement of IPCE greatly. In the past, it was demonstrated that the molecular structures of sensitizers have a significant influence on the photovoltaic performance of $\eta_{\mathrm{LHE}}$ and $\eta_{\mathrm{inj}}$ through influencing their Photophysical and electrochemical properties. The IPCEs for DSSCs based on the three dyes are presented in Fig. 6. As shown in Fig. 6, it is observed obviously that two peaks are located in the range of 400-500nm and 600-700nm, respectively, which is consistent with UV-visible absorption spectra of the three dyes.

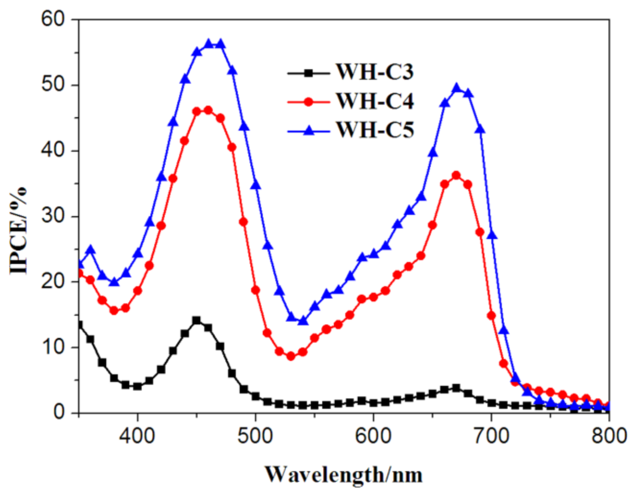


**Fig. 6** Action spectra of monochromatic incident photon-to-current conversion efficiency (IPCE) for DSSCs based on **WH-C3**, **WH-C4** and **WH-C5**. Black: **WH-C3**, red: **WH-C4**, and blue: **WH-C5**.

It is clear that **WH-C4** and **WH-C5** possess two nearly strong IPCEs values corresponding to Soret and Q absorption bands. In contrast, the maximum IPCE value of the Soret band of **WH-C3** is approximately three times as large as that of Q absorption band. It was explained by the fact that the introduction of strong electron-withdrawing 2,4,6-triphenyl-1,3,5-triazine is unfavourable to intramolecular charge transfer from HOMO to LUMO. As a matter of fact, the conclusion was demonstrated through utilizing a similar acceptor-π-donor-π-acceptor structure. **LW12** and **LW13** with the symmetrical acceptor-π-donor-π-acceptor structure showed inferior power conversion efficiencies compared to **LD14** with D-π-A structure.[43] Compared with **WH-C3**, the maximum IPCEs of Soret bands of **WH-C4** and **WH-C5** dye were increased by 291% and 229%, respectively. Additionally, although **WH-C5** dye has the weakest absorption at Soret and Q absorption bands in comparison with **WH-C3** and **WH-C4**, the DSSCs based on **WH-C5** exhibit optimal

IPCE. It may be caused by the higher $\eta_{inj}$ resulting from a higher LUMO level.

The current density-voltage (I-V) characteristic of the DSSCs sensitized by **WH-C3**, **WH-C4** and **WH-C5** is displayed in Fig. 7 with the corresponding detailed photovoltaic performance parameters listed in Table 2. Under standard global air mass 1.5 solar conditions, the **WH-C3** sensitized cell gave a short circuit photocurrent density ($J_{sc}$) of 2.50 mA cm$^{-2}$, an open circuit voltage ($V_{oc}$) of 514.57 mV, and a fill factor (*FF*) of 0.75, corresponding to an overall conversion efficiency ($\eta$) of 0.97%. The low $J_{sc}$ of **WH-C3** might be attributed to the following three reasons: Firstly, the low dye absorbed amount for **WH-C3** should be mainly responsible for the low IPCE and $J_{sc}$. Secondly, the **WH-C3** molecule with planar 2,4,6-triphenyl-1,3,5-triazine moiety is liable to aggregate and form self-quenching, leading to the low $\eta_{LHE}$ and IPCE. Finally, acceptor-π-donor-π-acceptor structure of **WH-C3** with electron-withdrawing groups on both sides of porphyrin ring was thought to be detrimental to intermolecular charge transfer and eventually influenced electron injection efficiency, which resulted in low IPCE and short circuit current. Actually, the fact that D-π-A structure is superior to A-π-A structure in porphyrin dye molecules has been demonstrated through theoretical calculations at the density functional B3LYP level.[44, 45] Under the same conditions, the DSSCs for **WH-C4** and **WH-C5** with incorporation of carbazole and triphenylamine as additional donor at the meso-position opposite to the anchoring benzoic acid group showed $J_{sc}$ of 10.07 and 11.43 mAcm$^{-2}$, $V_{oc}$ of 609.81 and 633.84 mV, and *FF* of 0.72 and 0.69, corresponding to $\eta$ of 4.40% and 5.00%, respectively. Apparently, $J_{sc}$ of DSSCs based on the three sensitizers increases with electron-donating ability of groups suspending at the meso-position opposite to anchoring group in the order of **WH-C3** < **WH-C4** < **WH-C5**, which is consistent with the trend of IPCEs.[46] In comparison with **WH-C3**, the $J_{sc}$ of **WH-C4** and **WH-C5**-sensitized solar cells is enhanced by 303% and 357%, respectively. So it has been well documented that the incorporation of electron-donating donor is beneficial to intramolecular charge transfer and improves the short circuit current dramatically. At the same time, the higher dye loading amount of **WH-C4** and **WH-C5** could be another cause of their higher $J_{sc}$. In addition, as seen from Table 2 and Fig. 7, the $V_{oc}$ of the devices sensitized by the three porphyrin dyes follows the order: $V_{oc}$（**WH-C5**）> $V_{oc}$(**WH-C4**) > $V_{oc}$(**WH-C3**).

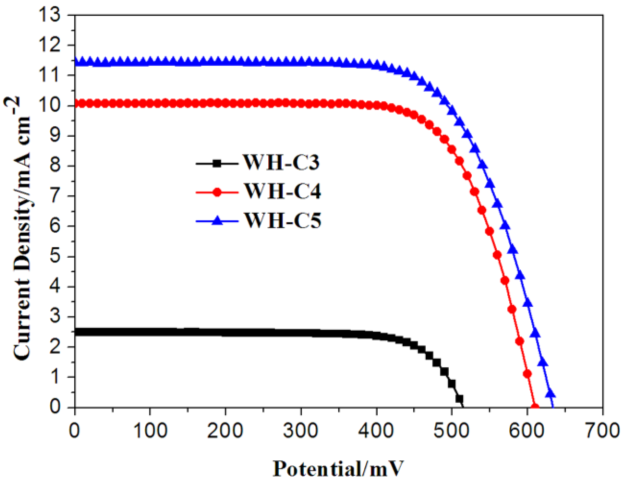


**Fig. 7** Current-voltage characteristics of DSSCs sensitized with **WH-C3**, **WH-C4** and **WH-C5** under AM 1.5 G simulated solar light (100 mW $cm^{-2}$). Black: **WH-C3**, red: **WH-C4**, and blue: **WH-C5**.

**Table 2.** The photovoltaic performance parameters of the DSSCs employing **WH-C3**, **WH-C4** and **WH-C5** under AM 1.5 G simulated solar light (100 mW $cm^{-2}$).

| **Dye** | $V_{oc}$/mV | $J_{sc}$/mA $cm^{-2}$ | *FF* | $\eta$/% | $R_{rec}/\Omega$ | $\tau_e$/ms |
|---|---|---|---|---|---|---|
| **WH-C3** | 514.57 | 2.50 | 0.75 | 0.97 | 14.26 | 2.04 |
| **WH-C4** | 609.81 | 10.07 | 0.72 | 4.40 | 17.75 | 27.99 |
| **WH-C5** | 633.84 | 11.43 | 0.69 | 5.00 | 39.41 | 37.97 |

From the perspective of molecular structure, the different $V_{oc}$ may be ascribed to vast differences between donor structures. Planar 2,4,6-triphenyl-1,3,5-triazine in **WH-C3** not only easily aggregates, but also weakly suppresses charge recombination between the electron injected into the conduction band of $TiO_2$ and $I_3^-$ at the vicinity of $TiO_2$. By contrast, carbazole and triphenylamine have a larger steric hindrance, preventing electron recombination which results in their higher $V_{oc}$.

**2.5. Electrochemical impedance spectroscopy (EIS)**

To further investigate and elucidate the photovoltaic results and obtain more interfacial charge transfer information of the DSSC with the different dyes, electrochemical impedance spectroscopy (EIS) was also performed in the dark under a forward bias of -0.6V. The Nyquist and Bode plots for **WH-C3**, **WH-C4** and **WH-C5** are shown in Fig. 8. From the Nyquist plots (Fig. 8(a)), in the high frequency range over $10^6$ Hz, the impedance is dominated by the ohmic serial resistance ($R_s$) of the dummy cell owing to the square resistance of FTO glass substrate, where the phase is zero.[5, 40] As seen in Fig. 8(a), the first semicircle is assigned to impedances related to charge transport at the electrolyte/counter electrode interface. In the middle frequency range, the large semicircle is ascribed to the electron recombination resistance ($R_{rec}$) and chemical capacitance at the working electrode /electrolyte.[47, 48] It is obvious that the semicircle based on different dyes is in the order of **WH-C3** < **WH-C4** < **WH-C5**, indicating that the electron recombination resistance augments from **WH-C3** to **WH-C5**.[5] It is well known that the photovoltage of a DSSC is intrinsically determined by the potential difference between the quasi Fermi level of $TiO_2$ and the redox potential of the electrolyte.[49] As a matter of fact, the $V_{oc}$ can be affected by following two factors: a) the shift of the $TiO_2$ conduction band edge; b) the degree of electron recombination reaction.[49] Based on the above conclusions, the order of the $V_{oc}$(**WH-C3** < **WH-C4** < **WH-C5**) could be attributed to different electron recombination resistances caused by different donors. The larger the semicircle is, the slower the recombination kinetics is. It is observed that the **WH-C5** with classical triphenylamine donor presented the highest recombination resistance. In the Bode phase plots Fig. 8(b), the middle-frequency peak stands for the charge-transfer process of injected electrons in $TiO_2$ corresponding to the first semicircle in Nyquist plots. The Bode phase plots likewise demonstrate the differences in the $R_{rec}$. Electron lifetime calculated through the relation $\tau_e = 1/(2\pi f)$ (f is the peak frequency of middle-frequency range in EIS Bode plot) [50] can effectively explain the higher $V_{oc}$ of **WH-C5**-sensitized solar cells compared with that of **WH-C3** and **WH-C4**. Electron lifetime $\tau_e$ was determined to be 2.04, 27.99 and 37.97 ms, for **WH-C3**, **WH-C4** and **WH-C5**, respectively. The higher electron lifetime $\tau_e$ observed from **WH-C5** indicated more effective repression of the charge recombination back reaction, which could be reflected in the improvements of $V_{oc}$, resulting in improved device efficiency. To summarise, it has been demonstrated that the incorporation of triphenylamine donor can act as blocking layer through suppression of recombination reaction between the electron injected into the conduction band of $TiO_2$ and $I_3^-$ at the vicinity of $TiO_2$.

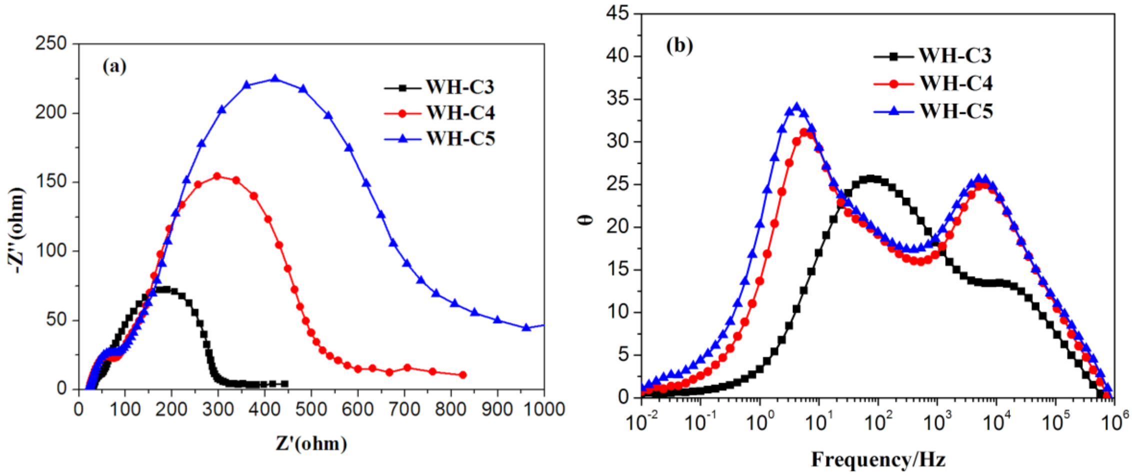


**Figure 8.** Electrochemical impedance spectroscopy (EIS) for DSSCs based on the sensitizers. (a) Nyquist plots; (b) Bode phase plots in the dark under a forward bias of -0.6 V.

## 3. Conclusions

In conclusion, three push-pull porphyrins with different electron-donating ability donors were designed and synthesized for monolithic dye-sensitized solar cells based on carbon/graphite counter electrodes. We have systematically investigated the effect of different electron-donating ability organic groups on the photovoltaic performance of the porphyrin-sensitized solar cells through photophysical, electrochemical, photocurrent -voltage curve, monochromatic incident photon-to-current conversion efficiency curve and electrochemical impedance spectroscopy characterization methods. The open circuit voltage and short circuit photocurrent density of the devices sensitized by the three porphyrin dyes follows the order: **WH-C5** > **WH-C4** > **WH-C3**. Under standard global air mass 1.5 solar conditions, the highest power conversion efficiency was achieved by the **WH-C5** sensitized solar cell, which gave a short circuit photocurrent density ($J_{sc}$) of 11.43 mA $cm^{-2}$, an open circuit voltage ($V_{oc}$) of 633.84 mV, and a fill factor (ff) of 0.69, corresponding to an overall conversion efficiency ($\eta$) of 5.00%. In a word, it has been demonstrated that the incorporation of different donors can have a profound impact on the photovoltaic performance of the porphyrin-sensitized solar cells. The present study could provide guidance role for the rational design of highly efficient porphyrin sensitizers.

## 4. Experimental

### 4.1. Materials

All reagents and solvents were obtained from commercial sources and used without further purification unless otherwise noted. THF and toluene was dried over sodium/benzophenone and freshly distilled before use. DMF used for formylation was dried over enough $P_2O_5$ for several hours and distilled under reduced pressure. Column chromatography of all the products was performed on silica gel (Kanto, Silica Gel 60N, spherical, 200–300 mesh), and some were further purified by recrystallization.

### 4.2. Preparation of platinized carbon paste

Platinized carbon paste was prepared as described elsewhere.[40] 2 g carbon black powders (particle size: 30 nm) and $H_2PtCl_6$ (Sigma) with a predetermined Pt/carbon black weight ratio were added into 20 ml isopropanol solution (Sigma) under continue stirring for 30 min, and then the paste was sintered for 30 min at 380 ◦C in furnace to thermally deposit the Pt nanoparticles on the surface of carbon black, followed by mixing with graphite powders (particle size: 1.3 μm) with a predetermined graphite/carbon black weight ratio. Finally, 1 g of 20 nm $ZrO_2$ nanopowders (Sigma) and 1 g of hydroxypropyl cellulose (Sigma) were added into a 30 ml terpineol solution. The platinized carbon material paste was obtained after stirring vigorously using ball milling for 2 h.

### 4.3. Synthesis

**4-iodo-N,N-diphenylaniline (1)**

Compound **1** was prepared according to literature procedure.[51, 52] To the solution of triphenylamine(1g, 4mmol) in 100mL HOAc were KI(0.332g, 2mmol) and $KIO_3$(0.428g, 2mmol) and was refluxed under dinitrogen for 14 h. The progress of the reaction was monitored with TLC. After finishing reacting, saturated $NaHSO_3$(aq) were added slowly into the reaction flask until the reaction solution turned from reddish brown to colourless. After extraction with DCM, The combined extracts were dried over anhydrous $MgSO_4$and the solvent was removed under reduced pressure. The residue was purified by column chromatography (silica gel) using petroleum ether as eluent to give a white solid **1**(1.128g, 76%). $^1$HNMR ($CDCl_3$, 600MHz) $\delta_H$ 7.49 (d, $J$ = 8.82Hz, 2H), 7.25 (t, $J$ = 7.89Hz, 4H), 7.07 (d, $J$ = 7.62Hz, 4H), 7.03 (t, $J$ = 7.35Hz, 2H), 6.82 (d, $J$ = 8.76Hz, 2H). $^{13}$C NMR ($CDCl_3$, 600 MHz) $\delta_C$ 147.3, 138.0, 129.4, 129.2, 125.3, 124.2, 123.3. APCI-MS: m/z calcd for $C_{18}H_{14}IN$ 371, found 371 $[M]^+$.

**2-(4-iodophenyl)-4,6-diphenyl-1,3,5-triazine (2)**

Compound **2** was prepared according to literature procedure.[53] A Schlenk tube was charged with CuI (11mg, 0.058mmol, 5.0 mol%), 2-(4-bromophenyl)-4,6-diphenyl-1,3,5-triazine(450mg, 1.159mmol), NaI (347mg, 2.318mmol), briefly evacuated and backfilled with argon. Ethylenediamine(8 μL, 0.116mmol, 10 mol%) and dioxane (2.0 mL)were added under argon. The Schlenk tube was sealed with a Teflon valve and the reaction mixture was stirred at 110 ℃ for 24 h. The resulting suspension was allowed to reach room temperature, diluted with 30% aq ammonia (5 mL), poured into water (20 mL), and extracted with dichloromethane (3×20 mL).The combined organic phases were dried over $Na_2SO_4$ and the solvent was removed under reduced pressure. The residue was purified by column chromatography (silica gel) using petroleum ether as eluent to give a white solid **2** (356mg, 70.6%). $^1$H NMR ($CDCl_3$, 600 MHz) $\delta_H$ 8.77 (d, *J* = 7.1 Hz, 4H), 8.65 (d, *J* = 8.5 Hz, 2H), 7.72 (d, *J* = 8.5 Hz, 2H), 7.65 (t, *J* = 7.2 Hz, 2H), 7.60 (t, *J* = 7.3 Hz, 4H). $^{13}$C NMR ($CDCl_3$, 600 MHz) $\delta_C$ 171.7, 170.8, 136.0, 135.2, 132.7, 131.9, 130.5, 129.0, 128.7, 127.5. APCI-MS: m/z calcd for $C_{21}H_{14}IN_3$ 435, found 435 $[M]^+$.

**9-ethyl-9H-carbazole (3)**

Compound **3** was prepared according to modified conditions of literature procedure.[54] Potassium hydroxide (42 g, 750mmol) was dissolved in DMF (200 ml) for 20min and then carbazole (19.8g, 120mmol) was added into the above solution and stirred for 40min. Subsequently, bromoethane (19.62 g, 180mmol) in 50ml DMF was stepwise added into the above solution and stirred overnight at RT. After being poured into 1L deionized water, the white precipitate appeared, stilled for 30 min, filtered and washed several times with cool water. The resulting precipitate was subjected to recrystallization from ethanol, giving white solid (21.36 g, 92.4%). $^1$HNMR ($CDCl_3$, 400MHz) $\delta_H$ 8.06 (d, *J* = 7.76 Hz, 2H), 7.42 (t, *J* = 8.2 Hz, 2H), 7.33(d, *J* = 8.2 Hz, 2H), 7.19 (t, *J* = 7.88 Hz, 2H), 4.25 (q, *J* = 7.2 Hz, 2H), 1.34 (t, *J* = 7.24 Hz, 3H). $^{13}$C NMR ($CDCl_3$, 400 MHz) $\delta_C$ 140.1, 125.7, 123.1, 120.5, 118.9, 108.5, 37.6, 13.9. APCI-MS: m/z calcd for $C_{14}H_{13}N$ 195, found 195 $[M]^+$.

**3-iodo-9-ethyl-9H-carbazole (4)**

A procedure similar to **1** was employed for the synthesis of **4** (1.137g,70.8%) from **3** (1g, 5mmol). $^1$HNMR ($CDCl_3$, 600MHz) δH 8.40 (s, 1H), 8.04 (d, *J* = 7.74 Hz, 1H), 7.71 (d, *J* = 8.52 Hz, 1H), 7.49 (t, *J* = 7.68 Hz, 1H), 7.40 (d, *J* = 8.22 Hz, 1H), 7.24 (d, *J* = 7.5 Hz, 1H), 7.20 (d, *J* = 8.52 Hz, 1H), 4.34 (q, *J* = 7.26 Hz, 2H), 1.41 (t, *J* = 7.29 Hz, 3H). $^{13}$C NMR ($CDCl_3$, 600 MHz) $\delta_C$ 139.9, 139.0, 133.8, 129.3, 126.4, 125.5, 121.7, 120.6, 119.3, 110.5, 108.7, 81.2, 37.6, 13.8. APCI-MS: m/z calcd for $C_{14}H_{12}IN$ 321, found 321 $[M]^+$.

**dipyrromethane (5)**

Compound **5** was prepared by adapting the literature procedure.[43, 55] Solid paraformaldehyde (3g, 90mmol) was added to pyrrole (150 mL, 2.16mol) and the solution degassed by stirring under reduced pressure and flushing with $N_2$. TFA (0.81 mL, 10.9 mmol) was added with vigorous stirring, and the reaction was allowed to proceed for 15 min at room temperature before NaOH (0.2M×100 mL). The product was extracted by DCM and washed with water (3×100 mL). The combined extracts were dried over anhydrous $MgSO_4$. After removal of DCM under diminished pressure, excess pyrrole was distilled out under reduced pressure. And then the crude product was purified by column chromatography eluted with ethyl acetate and petroleum ether mixture, giving the product as a colourless crystalline solid (6.97g, 53%). $^1H$ NMR ($CDCl_3$, 400 MHz) $\delta_H$ 7.54 (br. s, 7.54), 7.19 (s, 2H), 6.54 (m, 2H), 6.13 (m, 2H), 6.01 (m, 2H), 3.87 (s, 2H). $^{13}C$ NMR ($CDCl_3$, 400 MHz) $\delta_C$ 129.2, 117.5, 108.3, 106.6, 26.4. APCI-MS: m/z calcd for $C_9H_{10}N_2$ 146, found 146 $[M]^+$.

**1,3-Dioctoxybenzene (6)**

Compound **6** was prepared according to literature procedure.[20] A mixture of resorcinol (11 g, 0.1 mol), 1-bromooctane (69.6mL, 0.4mol) and $K_2CO_3$(69g, 0.5mol) was refluxed for 4 days in dry acetone (500mL).The solvent was removed under reduced pressure and extracted with EtOAc (3×100mL). The combined extracts were washed with water and dried over anhydrous $MgSO_4$. After removal of solvent under reduced pressure, the product was purified by column chromatography eluting with hexanes to give 1,3-di(octyloxy)benzene (26.5g, 79%). $^1H$ NMR ($CDCl_3$, 400 MHz) $\delta_H$ 7.13 (t, $J$ = 8.4 Hz, 1H), 6.46 (m, 3H), 3.92 (t, $J$ = 6.6 Hz, 4H), 1.79-1.72 (m, 4H), 1.47-1.40 (m, 4H), 1.35-1.23 (m, 16H), 0.88 (t, $J$ = 6.7 Hz, 6H). $^{13}C$ NMR ($CDCl_3$, 400 MHz) $\delta_C$ 160.4, 129.7, 106.7, 101.5, 68.0, 31.8, 29.4, 29.3, 29.2, 26.1, 22.7, 14.1. APCI-MS: m/z calcd for $C_{22}H_{38}O_2$ 335, found 336 $[M+1]^+$.

**2,6-Dioctoxybenzenaldehyde (7)**

Compound **7** was prepared according to literature procedure.[20] A three-neck flask was equipped with an additional funnel and charged with compound **9** (10 g, 0.03 mol) and tetramethylethylenediamine (TMEDA) (1.15 mL) in 84 mL of tetrahydrofuran. The solution was degassed with dinitrogen for 15 min and cooled to 0oC, and then n-butyllithium (22.4 mL, 1.6 M solution in hexanes 0.036 mol) was added dropwise over 20 min and allowed to stir for 3 h. After warming to room temperature, dimethylformamide (DMF) (4.38 mL, 0.06 mol) was added dropwise, and the reaction was stirred for an additional 2 h. The reaction was quenched with water, and the mixture was extracted with ether (3×80 mL), dried over anhydrous $MgSO_4$, and the solvent was removed under reduced pressure. The product was recrystallized from hexanes to yield a white solid (8.67 g, 80% yield). $^1$H NMR ($CDCl_3$, 400 MHz) $\delta_H$ 10.54 (s, 1H), 7.37 (t, $J$ = 8.4 Hz, 1H), 6.52 (d, $J$ = 8.5 Hz 2H), 4.01 (t, $J$ = 6.5 Hz, 4H), 1.85-1.78 (m, 4H), 1.50-1.43 (m, 4H), 1.36-1.28 (m, 16H), 0.88 (t, $J$ = 6.9 Hz, 6H). $^{13}$C NMR ($CDCl_3$, 400 MHz) $\delta_C$ 189.2, 161.7, 135.5, 114.8, 104.5, 68.9, 31.8, 29.3, 29.2, 29.1, 26.0, 22.6, 14.1. APCI-MS: m/z calcd for $C_{23}H_{38}O_3$ 362, found 363 $[M+1]^+$.

**5,15-Bis(2,6-dioctoxyphenyl)porphyrin (8)**

Compound **8** was synthesized according to literature procedure.[20] To a degassed solution of dipyrromethane (6.04 g, 41.4 mmol) and compound **7** (15 g, 41.4 mmol) in DCM (5.4 L) was added trifluoroacetic acid (2.75 mL, 37.3 mmol). After the solution was stirred at 23 ℃ under dinitrogen for 4 h, DDQ (14.1 g, 62.1 mmol) was added and the mixture was stirred for an additional 1 h. The mixture was basified with $Et_3N$ (7 mL) and filtered through silica. The solvent was removed under reduced pressure and the residue was purified by column chromatography (silica gel) using DCM/hexanes = 1/2 as eluent. The product was recrystallized from MeOH/$CH_2Cl_2$ to give the product (6.07 g, 30.1%) as a purple powder. $^1$H NMR ($CDCl_3$, 400 MHz) $\delta_H$ 10.12 (s, 2H), 9.24 (d, *J* = 4.6 Hz, 4H), 8.96 (d, *J* = 4.5 Hz, 4H), 7.68 (t, *J* = 8.4 Hz, 2H), 7.00 (d, *J* = 8.5 Hz, 4H), 3.82 (t, *J* = 6.4 Hz, 8H), 0.95-0.87 (m, 8H), 0.85-0.78 (m, 8H), 0.66-0.59 (m, 8H), 0.56-0.50 (m, 28H), 0.48-0.40 (m, 8H), -2.99 (s, 2H). $^{13}$C NMR ($CDCl_3$, 400 MHz) $\delta_C$ 160.2, 147.7, 145.0, 130.8, 130.4, 130.0, 120.1, 111.6, 105.4, 103.9, 68.8, 31.3, 28.6, 25.3, 22.3, 13.8. APCI-MS: m/z calcd for $C_{64}H_{86}N_4O_4$ 975, found 976 $[M+1]^+$.

**5,15-Dibromo-10,20-bis(2,6-dioctoxyphenyl)porphyrin (9)**

Compound **9** was synthesized according to literature procedure.[56, 57] Compound **8** (4.836g,4.96mmol) was dissolved in chloroform (300mL) with pyridine (2.6mL).A solution of NBS (1.768g, 9.92 mmol) in chloroform (100mL) and pyridine (1.4 mL) was added dropwise at 0℃ over 30min. The reaction was stirred for 15min and then quenched with acetone (10mL). The solvents were removed under reduced pressure and the residue was purified by column chromatography (silica gel) using DCM/hexanes = 1/4(volume ratio) as eluent. The product was recrystallized from THF/MeOH to give the product (5.18g, 92.2%) as a purple powder. $^1$H NMR ($CDCl_3$, 400 MHz) $\delta_H$ 9.50 (d, *J* = 4.8 Hz, 4H), 8.78 (d, *J* = 4.6 Hz, 4H), 7.69 (t, *J* = 8.4 Hz, 2H), 6.97 (d, *J* = 8.4 Hz, 4H), 3.83 (t, *J* = 6.4 Hz, 8H), 0.98–0.91 (m, 8H), 0.84–0.76 (m, 8H), 0.69–0.56 (m, 8H), 0.53–0.48 (m, 28H), 0.46–0.37 (m, 8H), -2.59 (s, 2H). $^{13}$C NMR ($CDCl_3$, 400 MHz) $\delta_C$ 160.0, 151.5, 149.8, 132.9, 130.1, 120.8, 115.0, 105.2, 104.0, 68.6, 31.3, 28.6, 25.3, 22.2, 13.8. APCI-MS: m/z calcd for $C_{64}H_{84}Br_2N_4O_4$ 1133, found 1133 $[M]^+$.

**[5,15-Dibromo-10,20-bis(2,6-di-octoxyphenyl)porphinato] zinc(II) (10)**

Compound **10** was prepared under modified conditions of literature procedure.[20] A suspension of **9** (4g, 3.52 mmol) and $Zn(OAc)_2$•$2H_2O$ (6.476g, 35.2mmol) in a mixture of DCM (400mL) and MeOH (200 mL) was stirred at RT overnight. The reaction was quenched with water (100 mL), and the mixture was extracted with DCM (2×100mL). The combined extracts were washed with water and dried over anhydrous $MgSO_4$. The solvent was removed under reduce pressure to give the product (3.92g, 93.1%). $^1$H NMR ($CDCl_3$, 400 MHz) $\delta_H$ 9.62 (d, *J* = 4.6 Hz, 4H), 8.88 (d, *J* = 4.6 Hz, 4H), 7.69 (t, *J* = 8.4 Hz, 2H), 6.99 (d, *J* = 8.4 Hz, 4H), 3.83 (t, *J* = 6.4 Hz, 8H), 0.97–0.91 (m, 8H), 0.86–0.74 (m, 8H), 0.61–0.54 (m, 8H), 0.53–0.41 (m, 28H), 0.39–0.32 (m, 8H). $^{13}$C NMR ($CDCl_3$, 400 MHz) $\delta_C$ 159.9, 151.4, 149.7, 132.8, 130.0, 120.7, 114.9, 105.2, 103.9, 68.6, 31.3, 28.6, 25.2, 22.2, 13.8. APCI-MS: m/z calcd for $C_{64}H_{82}Br_2N_4O_4Zn$ 1197, found 1197 $[M+1]^+$.

**[5,15-Bis(2,6-di-octoxyphenyl)-10,20-Bis[(triisopropylsilyl)ethynyl]-porphinato] zinc(II) (11)**

Compound **11** was prepared according to literature procedure.[20] A mixture of the zinc complex of **10** (0.910g, 0.81 mmol), (triisopropylsilyl)acetylene (0.906mL, 4.08 mmol), $Pd(PPh_3)_2Cl_2$ (0.220g, 0.32 mmol), CuI (0.094g, 0.48 mmol), THF (60 mL) and $NEt_3$ (10mL) was refluxed at 65℃ for 4 h under dinitrogen. The solvent was removed under vacuum. The residue was purified by column chromatography(silica gel) using DCM/hexanes = 1/20 to as eluent to give the product (0.97 g, 85.7%) as a purple solid. $^1$H NMR ($CDCl_3$, 400 MHz) $\delta_H$ 9.66 (d, $J$ = 4.6 Hz, 4H), 8.86 (d, $J$ = 4.6 Hz, 4H), 7.66 (t, $J$ = 8.4 Hz, 2H), 6.98 (d, $J$ = 8.4 Hz, 4H), 3.81 (t, $J$ = 6.4 Hz, 8H), 1.48–1.41 (m, 42H), 0.99–0.86 (m, 8H), 0.79–0.70 (m, 8H), 0.58–0.51 (m, 8H), 0.51–0.45 (m, 28H), 0.44–0.33 (m, 8H). $^{13}$C NMR ($CDCl_3$, 400 MHz) $\delta_C$ 159.9, 152.0, 150.7, 131.7, 130.9, 130.8, 121.0, 114.9, 110.1, 105.4, 100.2, 96.5, 68.8, 31.2, 28.5, 25.2, 22.1, 19.1, 13.7, 11.9. APCI-MS: m/z calcd for $C_{86}H_{124}N_4O_4Si_2Zn$ 1399, found 1400 $[M+1]^+$.

**Compound WH-C3**

Compound **WH-C3** was prepared according to literature procedure.[56-58] To a solution of porphyrin **11** (98 mg, 0.07 mmol) in dry THF (20 mL) was added TBAF (1M in THF, 0.57 mL, 0.57 mmol). The solution was stirred at room temperature for 0.5 h. The mixture was concentrated and then extracted with $CH_2Cl_2/H_2O$. The organic layer was dried over anhydrous $MgSO_4$ and the solvent was removed under vacuum. The residue, 2-(4-iodophenyl)-4,6-diphenyl-1,3,5-triazine (33.5mg, 0.077mmol, 1.1eq), and 4-iodobenzoic acid (17 mg, 0.07mmol, 1.0eq) were dissolved in a mixture of THF (20 mL) and $Et_3N$ (4 mL) and degassed with $N_2$ for 10 min, and then $Pd_2(dba)_3$ (33 mg, 0.036 mmol) and $AsPh_3$ (88 mg, 0.29mmol) were added to the mixture. The solution was refluxed for 5 h under $N_2$ and the solvent was removed under reduced pressure. The residue was purified on a column chromatography (silica gel) using $CH_2Cl_2/CH_3OH$ = 20/1 as eluent. Recrystallization from $CH_2Cl_2$/EtOH gave a green solid (32.8mg, 31%). $^1$H NMR ($CDCl_3$/pyridine-d5, 600 MHz) $\delta_H$ 9.61

(d, $J$ = 4.4 Hz, 4H), 8.89 (d, $J$ = 4.2 Hz, 2H), 8.87 (d, $J$ = 4.6 Hz, 2H), 8.86 (d, $J$ = 4.4 Hz, 2H), 8.84 (d, $J$ = 4.7 Hz, 4H), 8.30 (dd, $J$ = 3.8 Hz, 4H), 8.02 (t, $J$ = 6.2 Hz, 4H), 7.95 (d, $J$ = 7.8 Hz, 2H), 7.73 (d, $J$ = 8.6 Hz, 2H), 7.71 (d, $J$ = 8.6 Hz, 2H), 7.63 (d, $J$ = 9.1 Hz, 4H), 7.60 (d, $J$=6.4 Hz, 2H), 7.50 (t, $J$=7.6 Hz, 2H), 7.04 (t, $J$=8.6 Hz,8H), 3.87 (t, $J$ = 6.4 Hz, 8H), 1.33–1.19 (m, 8H), 0.98–0.86 (m, 8H), 0.74–0.72 (m, 8H), 0.65–0.56 (m, 28H), 0.46–0.42 (m, 8H). $^{13}$C NMR ($CDCl_3$/pyridine-$d_5$, 400 MHz) $\delta_C$ 159.9, 151.5, 151.3, 150.7, 150.6, 150.5, 136.1, 132.5, 131.6, 131.5, 131.3, 131.0, 130.9, 130.3, 130.1, 129.9, 129.8, 129.7, 129.6, 129.0, 128.9, 128.6, 128.5, 127.8, 124.7, 123.4, 121.3, 121.2, 115.3, 115.0, 105.1, 99.7, 94.9, 94.7, 93.9, 68.5, 31.4, 29.2, 28.7, 28.6, 25.2, 22.3, 13.8. ESI-MS: m/z calcd for $C_{96}H_{101}N_7O_6Zn$: 1514; found 1514 $[M]^+$.

**Compound WH-C4**

Compound **WH-C4** was synthesized from 3-iodo-9-ethyl-9H-carbazole (25mg, 0.077mmol, 1.1eq) according to the procedure as described above for synthesis of **WH-C3**, giving a green solid (37.6mg, 38.4%). $^1$H NMR ($CDCl_3$/pyridine-d5, 600 MHz) $\delta_H$ 9.70 (d, $J$ = 4.3 Hz, 2H), 9.60 (d, $J$ = 4.3 Hz, 2H), 8.84 (d, $J$ = 4.4 Hz, 4H), 8.70 (s, 1H), 8.52 (s, 1H), 8.29 (d, $J$ = 8.0 Hz, 2H), 8.24 (d, $J$ = 7.6 Hz, 1H), 8.08 (d, $J$ = 8.2Hz, 1H), 8.02 (d, $J$ = 8.0 Hz, 2H), 7.71 (t, $J$ = 8.6 Hz, 2H), 7.53 (t, $J$ = 8.4 Hz, 2H), 7.46 (d, $J$ = 8.1 Hz, 1H), 7.03 (d, $J$ = 8.6 Hz, 4H), 4.43 (q, $J$ = 7.2 Hz, 2H), 3.87 (t, $J$ = 6.4 Hz, 8H), 1.49 (t, $J$ = 7.2 Hz, 3H), 1.32–1.21 (m, 8H), 0.99–0.86 (m, 8H), 0.77–0.69 (m, 8H), 0.63–0.57(m, 28H), 0.48-0.46 (m, 8H). $^{13}$C NMR ($CDCl_3$/pyridine-$d_5$, 600 MHz) $\delta_C$ 160.0, 151.7, 151.4, 150.6, 150.4, 140.4, 139.5, 131.7, 131.3, 130.9, 130.4, 130.0, 129.9, 129.6, 129.3, 126.0, 123.8, 123.4, 122.7, 121.5, 120.7, 119.3, 114.9, 108.7, 105.2, 101.1, 98.2, 97.0, 96.7, 68.5, 37.7, 31.4, 28.7, 28.6, 28.5, 25.3, 22.3, 17.8, 13.9. ESI-MS: m/z calcd for $C_{89}H_{99}N_5O_6Zn$: 1400; found 1400 $[M]^+$.

**Compound WH-C5**

Compound **WH-C5** was synthesized from 4-iodo-N,N-diphenylaniline (29mg, 0.077 mmol, 1.1eq) according to the procedure as described above for synthesis of **WH-C3**, giving a green solid (41 mg, 40.6%). $^1$H NMR ($CDCl_3$/pyridine-d5, 600 MHz) $\delta_H$ 9.60 (dd, *J* = 4.4, 4.3 Hz, 4H), 8.85 (d, *J* = 4.4 Hz, 2H), 8.83 (d, *J* = 4.3 Hz, 2H), 8.28 (d, *J* = 7.7 Hz, 2H), 8.00 (d, *J* = 7.7 Hz, 2H), 7.80 (d, *J* = 8.1 Hz, 2H), 7.71 (t, *J* = 8.4 Hz, 2H), 7.31 (t, *J* = 7.5 Hz, 4H), 7.24 (d, *J* = 5.8 Hz, 2H), 7.20 (d, *J* = 7.7 Hz, 4H), 7.18 (d, *J* = 7.9 Hz, 2H), 7.09 (t, *J* = 7.3 Hz, 2H), 7.03 (d, *J* = 8.5 Hz, 2H), 3.87 (t, *J* = 6.2 Hz, 8H), 1.30–1.26 (m, 8H), 0.98–0.94 (m, 8H), 0.80–0.77 (m, 8H), 0.65–0.60 (m, 28H), 0.50–0.44 (m, 8H). $^{13}$C NMR ($CDCl_3$/pyridine-$d_5$, 600 MHz) $\delta_C$ 159.8, 151.5, 151.2, 150.5, 150.4, 149.6, 147.6, 147.2, 132.3, 130.8, 130.3, 129.8, 129.7, 129.4, 124.8, 123.4, 123.3, 122.6, 121.0, 115.0, 105.0, 100.5, 98.6, 94.9, 92.9, 68.4, 31.4, 28.7, 28.6, 28.5, 25.2, 22.3, 13.9. ESI-MS: m/z calcd for $C_{93}H_{101}N_5O_6Zn$: 1450; found 1450 $[M]^+$.

**4.4. Spectral and electrochemical measurements**

UV-visible spectra were performed on PerKinElmer Lambda 950 spectrophotometer. $^1$H NMR and $^{13}$C NMR spectra were recorded on Bruker-AV400 spectrometers with 400MHz. The chemical shifts were recorded in parts per million (ppm) with TMS as the internal reference. ESI mass spectra were measured on Finnigan LCQ Advantage mass spectrometer. The cyclic voltammetrys (CVs) were carried out with a three-electrode system in an argon-purged electrolyte solution on PARSTAT 2273 Electrochemical Workstation. Cyclic voltammograms for porphyrin dyes were conducted with a three-electrode cell equipped with a BAS glassy carbon (0.07 $cm^2$) disk as the working electrode, a platinum wire as the auxiliary electrode, and a Ag/AgCl (saturated) reference electrode. The working electrode was polished with 0.03 μm alumina on felt pads (Buehler) and treated ultrasonically for 1 min before each experiment. The potential of the reference electrode was adjusted by recording the cyclic voltammogram for 0.01 M ferrocene in THF containing 0.1 M $TBAPF_6$.

**4.5. Device fabrication**

A compact layer of $TiO_2$ was deposited on the FTO-coated glass by spray pyrolysis deposition with di-isopropoxytitanium bis(acetyl acetonate) solution. Subsequently the mesoporous $TiO_2$ (particle size, 20 nm, PASOL HPW-18NR TiO2 nanopowders, JGC Catalysts and Chemicals Ltd., Japan) transparent electrodes, the spacer layer composed of 40 and 90-nm-sized zirconia particles, and a mesoscopic platinized graphite/carbon black electrodes were prepared by screen printing onto FTO-coated conducting glass layer by layer, which were sintered at 500℃, 500℃ and 400℃ for 30min, respectively. Then the working electrode was prepared by immersing $TiO_2$ film into the 0.2mM dye solution (in Toluene/EtOH = 1/1,v/v) containing chenodeoxycholic acid (CDCA, 0.4 mM) at 25℃ overnight. The cell was encapsulated by a 100μm thick spacer of the thermo-bonding polymer (Surlyn, DuPont) with sheet glass. After sealing, the liquid electrolyte was injected into the cell through the hole predrilled in the sheet glass, and then the hole was sealed with Surlyn polymer and cover glass. The liquid electrolyte consisted of 1.0 M 1,2-dimethylimidazolium iodide (DMPII), 0.03M iodine, 0.1M guanidinium thiocyanate and 0.5M tert-butylpyridine in a mixture of acetonitrile/valeronitrile (85: 15, v/v).

**4.6. Photovoltaic measurements**

Current-voltage (*I*-*V*) characteristics were measured with a Keithley 2400 source/meter and a Newport solar simulator (model 91160) giving light with AM 1.5 G spectral distribution, which was calibrated using a certified reference solar cell (Fraunhofer ISE) to an intensity 100 mW $cm^{-2}$. A black mask with a slightly smaller circular aperture (0.07 $cm^2$) than the active area of the square solar cell (0.25 $cm^2$) was applied on top of the cell. The incident photon-to-current conversion efficiency (IPCE) was measured using a 150W xenon lamp (Oriel) fitted with a monochromator (Cornerstone 260) as monochromatic light source. The illumination spot size was chosen to be slightly smaller than the active area of the DSSC test cells. IPCE photocurrents were recorded under short-circuit conditions using a Keithley 2400 source meter. The monochromatic photon flux was quantified by means of a calibrated silicon photodiode. Electrochemical impedance spectroscopy (EIS) of the symmetric cell was measured using PARSTAT 2273 Electrochemical Workstation in the frequency range 0.1 to $10^6$ Hz with 10 mV AC amplitude. The electrolyte used was the same as that used for the fully functional DSSCs. The distance between two electrodes was 45 μm and the active area was 0.8 $cm^2$.

**Acknowledgements**

The authors acknowledge the financial support by the Ministry of Science and Technology of China (863, No. SS2013AA50303), the National Natural Science Foundation of China (Grant No. 61106056), the fundamental Research Funds for the Central Universities (HUSTNY022), and Scientific Research Foundation for Returned Scholars, Ministry of Education of China. We also thank the Analytical and Testing Center of Huazhong University of Science and Technology [HUST] for NMR, MS, UV-vis absorption and emission spectra measurements.

## References

1 B. O'Regan and M. Gratzel, *Nature*, 1991, **353**, 737-740.

2 A. Hagfeldt, G Boschloo, L. Sun, L. Kloo and H. Pettersson, *Chem. Rev.*, 2010, **110**, 6595.

3 B. E. Hardin, H. J. Snaith and M. D. McGehee, *Nat. Photonics*, 2012, **6**, 162.

4 C. Grätzel and S. M. Zakeeruddin, *Mater. Today*, 2013, **16**, 11.

5 S. Zhang, X. Yang, Y. Numata and L. Han, *Energy Environ. Sci.*, 2013, **6**, 1443.

6 M. K. Nazeeruddin, F. De Angelis, S. Fantacci, A. Selloni, G. Viscardi, P. Liska, S. Ito, B. Takeru and M. Grätzel, *J. Am. Chem. Soc.*, 2005, **127**, 16835.

7 Y. Chiba, A. Islam, Y. Watanabe, R. Komiya, N. Koide and L. Han, *Japanese Journal of Applied Physics*, 2006, **45**, L638.

8 F. Gao, Y. Wang, D. Shi, J. Zhang, M. Wang, X. Jing, R. Humphry-Baker, P. Wang, S. M. Zakeeruddin and M. Grätzel, *J. Am. Chem. Soc.*, 2008, **130**, 10720.

9 L. Han, A. Islam, H. Chen, C. Malapaka, B. Chiranjeevi, S. Zhang, X. Yang and M. Yanagida, *Energy Environ. Sci.*, 2012, **5**, 6057.

10 B. G Kim, K. Chung and J. Kim, *Chem.-Eur. J.*, 2013, **19**, 5220.

11 C. W. Lee, H. P. Lu, C. M. Lan, Y. L. Huang, Y. R. Liang, W. N. Yen, Y. C. Liu, Y. S. Lin, E. W. G. Diau and C. Y. Yeh, *Chem.-Eur. J.*, 2009, **15**, 1403.

12 W. Zhou, B. Zhao, P. Shen, S. Jiang, H. Huang, L. Deng and S. Tan, *Dyes Pigments*, 2011, **91**, 404.

13 C.-Y. Lin, C.-F. Lo, L. Luo, H.-P. Lu, C.-S. Hung and E. W.-G. Diau, *J. Phys. Chem. C*, 2008, **113**, 755.

14 J. K. Park, J. Chen, H. R. Lee, S. W. Park, H. Shinokubo, A. Osuka and D. Kim, *J. Phys. Chem. C*, 2009, **113**, 21956.

15 M. V. Martínez-Díaz, G. de la Torre and T. Torres, *Chem. Commun.*, 2010, **46**, 7090.

16 L.-L. Li and E. W.-G. Diau, *Chem. Soc. Rev.*, 2013, **42**, 291.

17 M. Urbani, M. Grätzel, M. K. Nazeeruddin and T. s. Torres, *Chem. Rev.*, 2014, **114**, 12330.

18 Y. Wang, X. Li, B. Liu, W. Wu, W. Zhu and Y. Xie, *RSC Adv.*, 2013, **3**, 14780.

19 B. Liu, W. Zhu, Y. Wang, W. Wu, X. Li, B. Chen, Y.-T. Long and Y. Xie, *J. Mater. Chem.*, 2012, **22**, 7434.

20 A. Yella, H.-W. Lee, H. N. Tsao, C. Yi, A. K. Chandiran, M. K. Nazeeruddin, E. W.-G. Diau, C.-Y. Yeh, S. M. Zakeeruddin and M. Grätzel, *Science*, 2011, **334**, 629.

21 Y. Wang, B. Chen, W. Wu, X. Li, W. Zhu, H. Tian and Y. Xie, *Angew. Chem., Int. Ed.*, 2014, **53**, 10779.

22 S. Mathew, A. Yella, P. Gao, R. Humphry-Baker, B. F. Curchod, N. Ashari-Astani, I. Tavernelli, U. Rothlisberger, M. K. Nazeeruddin and M. Grätzel, *Nat. chem.*, 2014, **6**, 242.

23 N. Cai, S.-J. Moon, L. Cevey-Ha, T. Moehl, R. Humphry-Baker, P. Wang, S. M. Zakeeruddin and M. Grätzel, *Nano. lett.*, 2011, **11**, 1452.

24 H. N. Tsao, C. Yi, T. Moehl, J. H. Yum, S. M. Zakeeruddin, M. K. Nazeeruddin and M. Grätzel, *ChemSusChem*, 2011, **4**, 591.

25 N. Koumura, Z.-S. Wang, S. Mori, M. Miyashita, E. Suzuki and K. Hara, *J. Am. Chem. Soc.*, 2006, **128**, 14256.

26 J. Park, E. Lee, J. Kim and Y. Kang, *Notes*, 2013, **34**, 1533.

27 K. Hara, M. Kurashige, Y. Dan-oh, C. Kasada, A. Shinpo, S. Suga, K. Sayama and H. Arakawa, *New J. Chem.*, 2003, **27**, 783.

28 Z.-S. Wang, Y. Cui, Y. Dan-oh, C. Kasada, A. Shinpo and K. Hara, *J. Phys. Chem. C*, 2007, **111**, 7224.

29 T. Horiuchi, H. Miura, K. Sumioka and S. Uchida, *J. Am. Chem. Soc.*, 2004, **126**, 12218.

30 B. Liu, Q. Liu, D. You, X. Li, Y. Naruta and W. Zhu, *J. Mater. Chem.*, 2012, **22**, 13348.

31 D. Cao, J. Peng, Y. Hong, X. Fang, L. Wang and H. Meier, *Org. Lett.*, 2011, **13**, 1610.

32 C. Chen, J.-Y. Liao, Z. Chi, B. Xu, X. Zhang, D.-B. Kuang, Y. Zhang, S. Liu and J. Xu, *J. Mater. Chem.*, 2012, **22**, 8994.

33 C.-J. Yang, Y. J. Chang, M. Watanabe, Y.-S. Hon and T. J. Chow, *J. Mater. Chem.*, 2012, **22**, 4040.

34 F. Guo, J. He, S. Qu, J. Li, Q. Zhang, W. Wu and J. Hua, *RSC Adv.*, 2013, **3**, 15900.

35 H. Imahori, T. Umeyama and S. Ito, *Acc. Chem. Res.*, 2009, **42**, 1809.

36 J.-J. Kim, H. Choi, J.-W. Lee, M.-S. Kang, K. Song, S. O. Kang and J. Ko, *J. Mater. Chem.*, 2008, **18**, 5223.

37 T. Daeneke, A. J. Mozer, Y. Uemura, S. Makuta, M. Fekete, Y. Tachibana, N. Koumura, U. Bach and

L. Spiccia, *J. Am. Chem. Soc.*, 2012, **134**, 16925.

38 M. Wang, C. Grätzel, S. M. Zakeeruddin and M. Grätzel, *Energy Environ. Sci.*, 2012, **5**, 9394.

39 H. Wang, G Liu, X. Li, P. Xiang, Z. Ku, Y. Rong, M. Xu, L. Liu, M. Hu and Y. Yang, *Energy Environ. Sci.*, 2011, **4**, 2025.

40 G. Liu, H. Wang, X. Li, Y. Rong, Z. Ku, M. Xu, L. Liu, M. Hu, Y. Yang and P. Xiang, *Electrochimica Acta*, 2012, **69**, 334.

41 M. Xu, G. Liu, X. Li, H. Wang, Y. Rong, Z. Ku, M. Hu, Y. Yang, L. Liu and T. Liu, *Org.Electronics*, 2013, **14**, 628.

42 M. K. Nazeeruddin, A. Kay, I. Rodicio, R. Humphry-Baker, E. Müller, P. Liska, N. Vlachopoulos and M. Grätzel, *J. Am. Chem. Soc.*, 1993, **115**, 6382.

43 J. Lu, X. Xu, Z. Li, K. Cao, J. Cui, Y. Zhang, Y. Shen, Y. Li, J. Zhu and S. Dai, *Chem.-an Asian. J.*, 2013, **8**, 956.

44 R. Ma, P. Guo, H. Cui, X. Zhang, M. K. Nazeeruddin and M. Grätzel, *J. Phys. Chem. A*, 2009, **113**, 10119.

45 R. Ma, P. Guo, L. Yang, L. Guo, X. Zhang, M. K. Nazeeruddin and M. Grätzel, *J. Phys. Chem. A*, 2010, **114**, 1973.

46 Q.-Y. Yu, J.-Y. Liao, S.-M. Zhou, Y. Shen, J.-M. Liu, D.-B. Kuang and C.-Y. Su, *J. Phys. Chem. C*, 2011, **115**, 22002.

47 L. Han, N. Koide, Y. Chiba and T. Mitate, *Appl. Phys. Lett.*, 2004, **84**, 2433.

48 M. Itagaki, K. Hoshino, Y. Nakano, I. Shitanda and K. Watanabe, *Journal of Power Sources*, 2010, **195**, 6905.

49 K. Cao, J. Lu, J. Cui, Y. Shen, W. Chen, A. Getachewalemu, Z. Wang, H. Yuan, J. Xu and M. Wang,

*J. Mater. Chem. A*, 2014, **2**, 4945.

50 Z. Wan, C. Jia, Y. Duan, L. Zhou, Y. Lin and Y. Shi, *J. Mater. Chem.*, 2012, **22**, 25140.

51 Y. Wu, H. Guo, T. D. James and J. Zhao, *J. Org. Chem.*, 2011, **76**, 5685.

52 L.-L. Tan, L.-J. Xie, Y. Shen, J.-M. Liu, L.-M. Xiao, D.-B. Kuang and C.-Y. Su, *Dyes Pigments*, 2014, **100**, 269.

53 A. Klapars and S. L. Buchwald, *J. Am. Chem. Soc.*, 2002, **124**, 14844.

54 S. H. Kim, I. Cho, M. K. Sim, S. Park and S. Y. Park, *J. Mater. Chem.*, 2011, **21**, 9139.

55 M. Balaz, H. A. Collins, E. Dahlstedt and H. L. Anderson, *Organic & biomolecular chemistry*, 2009, **7**, 874-888.

56 S.-L. Wu, H.-P. Lu, H.-T. Yu, S.-H. Chuang, C.-L. Chiu, C.-W. Lee, E. W.-G. Diau and C.-Y. Yeh, *Energy Environ. Sci.*, 2010, **3**, 949.

57 T. Ripolles-Sanchis, B.-C. Guo, H.-P. Wu, T.-Y. Pan, H.-W. Lee, S. R. Raga, F. Fabregat-Santiago, J. Bisquert, C.-Y. Yeh and E. W.-G Diau, *Chem. Commun.*, 2012, **48**, 4368.

58 C.-P. Hsieh, H.-P. Lu, C.-L. Chiu, C.-W. Lee, S.-H. Chuang, C.-L. Mai, W.-N. Yen, S.-J. Hsu, E. W.-G Diau and C.-Y. Yeh, *J. Mater. Chem.*, 2010, **20**, 1127.

Graphical Abstract

Comparing with **WH-C3** and **WH-C4**, **WH-C5**-sensitized device shows a significantly enhanced $V_{oc}$ , $J_{sc}$ and power conversion efficiency ($\eta$).